Alteration of serum lipid profile, SRB1 loss, and impaired Nrf2 activation in *CDKL5* disorder

Alessandra Pecorelli[a,b], **Giuseppe Belmonte**[c], **Ilaria Meloni**[d], **Franco Cervellati**[c], **Concetta Gardi**[a], **Claudia Sticozzi**[c], **Claudio De Felice**[e], **Cinzia Signorini**[a], **Alessio Cortelazzo**[b], **Silvia Leoncini**[a,b], **Lucia Ciccoli**[a], **Alessandra Renieri**[d,f], **Henry Jay Forman**[g,h], **Joussef Hayek**[b,1], and **Giuseppe Valacchi**[c,i,1,*]

[a]Department of Molecular and Developmental Medicine, University of Siena, Siena, Italy

[b]Child Neuropsychiatry Unit, Azienda Ospedaliera Universitaria Senese, "Santa Maria alle Scotte" General Hospital, Siena, Italy

[c]Department of Life Sciences and Biotechnology, University of Ferrara, Ferrara, Italy

[d]Medical Genetics, University of Siena, Siena, Italy

[e]Neonatal Intensive Care Unit, Azienda Ospedaliera Universitaria Senese, "Santa Maria alle Scotte" General Hospital, Siena, Italy

[f]Genetica Medica, Azienda Ospedaliera Universitaria Senese, Siena, Italy

[g]Life and Environmental Sciences Unit, University of California at Merced, Merced, CA 95344, USA

[h]Andrus Gerontology Center of the Davis School of Gerontology, University of Southern California, Los Angeles, CA 90089, USA

[i]Department of Food and Nutrition, Kyung Hee University, Seoul, South Korea

Abstract

CDKL5 mutation is associated with an atypical Rett syndrome (RTT) variant. Recently, cholesterol homeostasis perturbation and oxidative-mediated loss of the high-density lipoprotein receptor SRB1 in typical RTT have been suggested. Here, we demonstrate an altered lipid serum profile also in *CDKL5* patients with decreased levels of SRB1 and impaired activation of the defensive system Nrf2. In addition, *CDKL5* fibroblasts showed an increase in 4-hydroxy-2-nonenal– and nitrotyrosine–SRB1 adducts that lead to its ubi-quitination and probable degradation. This study highlights a possible common denominator between two different RTT variants (*MECP2* and *CDKL5*) and a possible common future therapeutic target.

Keywords

Scavenger receptor class B type 1; Nuclear factor erythroid 2-related factor 2; 4-Hydroxy-2-nonenal; Nitrotyrosine; Inducible nitric oxide synthase; Oxidative stress; Free radicals

[*]Corresponding author. giuseppe.valacchi@unife.it (G. Valacchi).
[1]These authors supervised this work equally

Mutations in loci other than the methyl-CpG binding protein 2 (*MECP2*) gene, linked to the occurrence of the typical Rett syndrome (RTT) [1–3], have been described in individuals labeled as atypical RTT. Although they have some overlapping clinical features of RTT, several variations in severity of impairment and clinical course have been described [4]. Among these variants, the "early-onset seizure variant," initially described by Hanefeld in 1985 [5], has been associated with mutations in the X-linked cyclin-dependent kinase-like 5 (*CDKL5*) gene [6].

Approximately 100 *CDKL5* cases were previously reported worldwide by the International Foundation for *CDKL5* Research [7]. However, about 600 cases are known today to be present in the world [7], with a 1000% increase in the past 5 years, owing to the increase in familiarity of physicians and geneticists with *CDKL5* mutations.

Recent evidence indicates that cholesterol homeostasis is perturbed in *Mecp2*-null mice owing to mutation in the gene encoding squalene epoxidase (*SQLE*), a rate-limiting cholesterol biosynthesis enzyme [8]. Moreover, our previous study demonstrated higher serum cholesterol in *MECP2* patients (classical RTT), associated with an oxidative-mediated loss of scavenger receptor class B, type 1 (SRB1), a specific high-density lipoprotein (HDL) receptor [9], in fibroblasts isolated from *MECP2* patients [10]. These new observations have brought new insights into possible therapeutic targets for RTT, although these aspects have not been evaluated for the other RTT variant *CDKL5,* which represents about 5% of RTT patients.

Recently, the presence of systemic redox imbalance has been described among the RTT variants [11] although the molecular mechanism responsible for increased oxidative stress (OS) was not elucidated. One of the main mechanisms involved in the cellular antioxidant defense is the activation of the nuclear factor erythroid 2-related factor 2 (Nrf2 or NFE2L2) system, a major transcription factor for antioxidant and cytoprotective responses [12–14]. Upon OS, Nrf2 translocates into the nucleus and binds to electrophile response elements (EpRE's, also known as antioxidant response elements), increasing transcription of genes related to cellular defense [14]. Impaired Nrf2 activation has been suggested for several pathologies [15].

The present work was designed to evaluate the serum cholesterol profile in *CDKL5* patients. Then, using freshly isolated skin fibroblasts, a good model to study the molecular mechanisms involved in several pathologies [16], we determined Nrf2 activation and the expression (protein and mRNA) and oxidative post-translational modification of SRB1.

1. Materials and methods

1.1. Subjects

Sixteen patients (females; mean age 11.4±5.1 years, range 2–18) with *CDKL5* mutations were enrolled in this study. All the patients were consecutively admitted to the Rett Syndrome National Reference Center of the University Hospital of Siena (Azienda Ospedaliera Universitaria Senese). Thirty healthy control subjects were sex- and age-matched (females; mean age 13.6±5.3 years, range 5–22). The subjects examined in this

study were on a typical Mediterranean diet. Blood samplings in the control group were carried out during routine health checks or blood donations, whereas blood samples from patients were obtained during periodic clinical checkups. The study was conducted with the approval of the institutional review board and all informed consents were obtained from either the parents or the legal guardians of the enrolled patients.

1.2. Determination of serum lipid profile

Fasting venous blood was collected at 8:00–10:00 AM after an overnight fast. Sera were separated and analyzed for total cholesterol (TC), triglycerides (TG), low-density lipoprotein cholesterol (LDL-C), and HDL-C, using specific diagnostic kits (HDL-cholesterol plus third generation and LDL-cholesterol plus second generation, respectively; Cobas, Roche, Basel, Switzerland).

1.3. Human dermal fibroblast culture

After informed consent, 4-mm punch biopsies were obtained from four *CDKL5* patients and four healthy female control donors. Primary dermal fibroblasts were isolated from dermal tissue specimens, as previously described [10]. Fibroblasts at low passage were employed for the analyses.

1.4. Cell treatments and protein extraction

CDKL5 and healthy control fibroblasts (80–90% confluence) were seeded in 100-mm dishes and treated with 4-hydroxy-2-nonenal (HNE; 5 μM) or H_2O_2 (100 μM) for various times. Total, cytoplasmic, and nuclear extracts were obtained as previously described [17,18].

1.5. Immunoprecipitation

For immunoprecipitation, 500 μg of cellular protein was incubated with 5 μg of SRB1 antibody (Millipore Corp., Billerica, MA, USA) and the assay was performed as previously described [10].

1.6. Western blotting

Protein concentrations were determined by the Bradford assay (Bio-Rad Laboratories, Segrate, Italy) and 40 μg of proteins was separated on 10% SDS–PAGE gels and transferred to nitrocellulose membranes. After blocking, the membranes were incubated with the primary antibodies: 4-hydroxy-2-nonenal, nitrotyrosine, SRB1 (Millipore), Nrf2 (Cell Signaling Technology, Danvers, MA, USA), and GCLC (gift from Professor H.J. Forman). After secondary antibody incubation, the membranes were exposed to enhanced chemiluminescence reagents and the bands visualized by autoradiography. Band densitometry was performed using ImageJ software. In some cases, membranes were stripped and reprobed with β-actin antibody (Millipore). Results were normalized with the respective loading control (Ponceau or β-actin).

1.7. Immunofluorescence

Healthy control and *CDKL5* fibroblasts were seeded on cover-slips at a density of 2×10^4 cells/cm^2. For Nrf2 nuclear translocation, fibroblasts were treated for 1 h with H_2O_2 (100

μM) or HNE (5 μM). After fixation and blocking, the cells were incubated overnight with the primary antibodies: 4-hydroxy-2-nonenal, nitrotyrosine, SRB1 (Millipore), and Nrf2 (Cell Signaling Technology). Then, the cells were incubated with Alexa Fluor 568 and Alexa Fluor 488 antibodies (Life Technologies Italia, Monza, Italy). The nuclei were stained with DAPI. Negative controls were generated by omitting the primary antibodies. Images were acquired with a Leica AF CTR6500HS microscope (Microsystems). For automatic visualization of colocalized fluorescence signals, ImageJ software was used, and the threshold values were determined and set for the two channels, so as to eliminate background noise. White spots represent positive correlation (colocalization).

1.8. Reverse transcription quantitative real-time PCR

Total RNA was extracted from fibroblasts using the RNeasy mini kit (Qiagen, Hilden, Germany) and RT-qPCR was performed as previously reported [19]. Primer sequences were SRB1, fwd 5′-GAATTCGCCTTTCGTCCCCG-3′, rev 5′-TTGAAGGACAGGCTACTGGG-3′; GCLC, fwd 5′-ACAGGACCAACCGGACTTTT-3′, rev 5′-CAGACTTC ACGTTTCCCTGC-3′; and GAPDH (internal standard), fwd 5′-TGAC GCTGGGGGCTGGCATTG-3′, rev 5′-GGCTGGTGGTCCAGGGGTCT-3′. After normalization to more stable GAPDH mRNA, the folds of variation were determined with respect to the control, using the formula $2^{-\Delta\Delta Ct}$, where ΔC_t is (gene of interest C_t) – (GAPDH C_t) and $\Delta\Delta C_t$ is (ΔC_t experimental) – (ΔC_t control).

1.9. Oil red O staining

Fibroblasts were seeded on coverslips and incubated with 50 μg/ml HDL for 24 h and then fixed for 30 min at room temperature with 4% paraformaldehyde. Fixed cells were stained with freshly prepared oil red O solution for 30 min at 60 °C. The nuclei were stained with hematoxylin for 5 min. Images were acquired with a Leica AF CTR6500HS microscope (Microsystems). To quantify staining, oil red O was extracted from cells and the absorbance was then measured at 492 nm. Cell protein concentrations were determined and absorbance values were normalized to protein.

1.10. Statistical analysis

Results are expressed as means±SD. Statistical comparisons were performed using the Student *t* tests. A *P* value of <0.05 was considered statistically significant.

2. Results

2.1. Serum lipid profile alteration in CDKL5 patients

As shown in Table 1, *CDKL5* patients present an altered lipid profile. Indeed, TC (194.6±24.7 mg/dl), LDL-C (103.5±16.4 mg/dl), and HDL-C (67.9±17.9 mg/dl) levels in *CDKL5* patients were significantly higher than in the control group (162.3±14.6, 87.6±11.3, 49.8±6.3 mg/dl, respectively; *P*<0.05). However, TG levels, although higher in the *CDKL5* group (88.9±33.8 mg/dl), were not significantly different from controls (80.2±20.2 mg/dl).

2.2. CDKL5 fibroblasts present low levels of SRB1 protein

The alterations in the serum lipid profile observed in *CDKL5* patients prompted us to analyze the SRB1 protein level, given its critical role in lipoprotein metabolism and cholesterol homeostasis [9]. As shown in Fig. 1A, in *CDKL5* fibroblasts we observed a significant decrease in SRB1 protein level (about 37%) compared to control cells.

2.3. Upregulation of SRB1 mRNA expression in CDKL5 fibroblasts

To explore the possible mechanism by which SRB1 is down-regulated in *CDKL5* fibroblasts, the transcription level of SRB1 was analyzed. As shown in Fig. 1B, SRB1 mRNA levels were significantly increased (about sixfold) in *CDKL5* cells compared to the control cells.

2.4. Increased oxidative marker levels in CDKL5 fibroblasts

One mechanism that can lead to the loss of proteins is oxidative modification, which can mark them for degradation [20,21]. Therefore we analyzed the presence of oxidative markers in *CDKL5* fibroblasts. As is shown in Fig. 2, immunoblotting analysis revealed several reactive bands for HNE–protein adducts (HNE–PA; Fig. 2A, left) and nitrotyrosine protein adducts (NT–PA; Fig. 2A, right) in *CDKL5* cell lysates, whereas fewer and/or weaker bands were observed in control cells. Oxidatively modified proteins were detected in both the high and the lower molecular weight bands, but showed a stronger intensity between 50 and 250 kDa for HNE–PA (Fig. 2A, left) and between 50 and 100 kDa for NT–PA (Fig. 2A, right). Densitometry analysis of all the bands present in each lane showed a significant increase in both HNE–PA and NT–PA levels in *CDKL5* fibroblasts (Fig. 2A, bottom). Data were also confirmed by immunofluorescence (Fig. 2B).

2.5. Inducible nitric oxide synthase upregulation in CDKL5 fibroblasts

To understand the source of NT–PA, we assessed the expression of inducible nitric oxide synthase (iNOS) protein. As shown in Fig. 2C, *CDKL5* fibroblasts had a markedly increased expression of iNOS (threefold).

2.6. SRB1 oxidative posttranslational modifications affect cholesterol uptake in CDKL5 fibroblasts

After confirming the evidence of cellular nitrosative/oxidative imbalance with increased oxidative posttranslational modifications in *CDKL5* patients, we examined whether SRB1 can form adducts with HNE and NT. As evident from Fig. 3A (top), immunoprecipitation/ Western blotting assays revealed the heightened occurrence of HNE– and NT–SRB1 adducts in *CDKL5* fibroblasts, also confirmed by double immunofluorescence (Fig. 3A, bottom). In particular, green fluorescence for SRB1 confirmed its lower levels in *CDKL5* cells (left column) with an associated increase in HNE–PA levels (central column, red fluorescence). A clear colocalization of SRB1 with HNE–PA was evident in the merged images (right columns, yellow color and white spots), indicating the formation of HNE–SRB1 adducts in *CDKL5* fibroblasts.

In addition, we evaluated whether the ubiquitination process was involved in the posttranslational modifications of SRB1. As shown in Fig. 3B, immunoprecipitation assays show a clear interaction between ubiquitin and SRB1, data confirmed also by immunofluorescence (Fig. 3B, bottom). Merged images (yellow color) show the association of SRB1 and ubiquitin; in particular the areas of colocalization, indicated by white spots, clearly demonstrated more overlap of the two signals in *CDKL5* fibroblasts.

The cellular ability to take up HDL-C was determined in control and *CDKL5* cells. As shown in Fig. 3C, *CDKL5* cells showed an impaired ability to take up cholesterol (lipid droplets in red) with respect to the control cells. This difference was statistically significant, as quantified on the left (Fig. 3C).

2.7. Aberrant Nrf2 activation in CDKL5 fibroblasts

As the stability and nuclear translocation of the transcription factor Nrf2 increase in response to OS and are critical in the regulation of intracellular redox balance [12–14], we examined Nrf2 protein levels and translocation. As shown in Fig. 4A, in *CDKL5* fibroblasts Nrf2 protein expression was 56% lower than in control cells. In addition, we evaluated the cytoplasmic (data not shown) and nuclear levels of Nrf2 in control and *CDKL5* cells after challenging them for 1 h with two well-known Nrf2 activators, i.e., H_2O_2 and HNE. As shown in Fig. 4B, *CDKL5* cells had lower nuclear levels of Nrf2 and were not able to further induce Nrf2 translocation after H_2O_2 or HNE exposure. Instead, control cells showed a clear ability to induce Nrf2 translocation after the different stimulations (Fig. 4B).

The data were also confirmed by immunofluorescence, as shown in Fig. 4C; control cells exhibited higher levels of both cytoplasmic and nuclear Nrf2 than did *CDKL5* cells. Furthermore, when the cells were challenged with H_2O_2 or HNE, *CDKL5* showed a clearly lower response in terms of Nrf2 activation.

The aberrant activation of Nrf2 was further confirmed by analyzing the expression (mRNA and protein) of *GCLC,* a gene regulated by Nrf2 [22]. As is depicted in Fig. 5A, *CDKL5* cells showed a lower level of GCLC mRNA and treatment with HNE did not affect its expression after 12 h. This effect was also noticed for GCLC protein levels, as shown in Fig. 5B. Control cells were able to increase both mRNA and protein levels of GCLC after the challenge with HNE (Fig. 5A and 5B).

3. Discussion

Mutations in *CDKL5,* a gene located on the X chromosome and encoding cyclin-dependent-like kinase 5, have been identified in individuals with an atypical variant of RTT, a severe neurologic disorder linked to mutations in the X-linked *MECP2* gene [1–6]. *CDKL5* patients show early-onset intractable seizures and a wide variety of other symptoms, such as neurodevelopmental impairment, intellectual disability, and motor delay [23].

Evidence indicates that CDKL5 binds to and phosphorylates MeCP2 in vitro, suggesting a possible molecular link between *CDKL5* disorder and typical RTT [24]. Therefore, some similarities between typical RTT and *CDKL5* are related not only to the clinical features, but

also to the cellular and molecular mechanisms. For instance, a recent study has shown that neurons with *CDKL5* mutation and neurons with *MECP2* mutation have a common altered gene, *GluD1,* which is involved in neuronal differentiation [25].

In the present work, we have demonstrated that the loss of SRB1 and the altered serum lipid profile previously noticed in *MECP2* patients [10] are present also in *CDKL5* subjects. Because of their strictly controlled diet, this increase in serum cholesterol levels should be the consequence of an altered lipid metabolism linked to the diseases.

In addition, cholesterol has multiple roles in the nervous system, from membrane trafficking to myelin formation, along with synapsis formation [26]. Therefore, the understanding of cholesterol metabolism has become an emerging area in several neurological diseases.

In fact, very recently, in an elegant study published in *Nature Genetics,* Buchovecky and colleagues [8] showed that cholesterol metabolism is perturbed in the brain and liver of *Mecp2*-null male mice, suggesting that cholesterol homeostasis maintenance could be disrupted in RTT and deeply involved in the onset of the disease. In addition, in a recent work we have also shown that 3-hydroxy-3-methylglutaryl-CoA reductase, the rate-limiting enzyme of the cholesterol biosynthetic pathway [27,28], was significantly lower in fibroblasts isolated from RTT patients [29], confirming not only the "cholesterol pathway" aberration, but also the reliability of the model used (skin fibroblasts isolated by biopsy). Indeed, in the present work we have found a significant increase in HDL and LDL levels in *CDKL5* patients and this was associated with loss of SRB1. In fact, SRB1 is involved in the binding of HDL and also LDL, thereby promoting selective tissue uptake of cholesterol [9]. In addition, SRB1 is also implicated in several other cellular processes, such as recognition of pathogens and apoptotic cells as well as uptake of lipid-soluble antioxidants [9], all features found altered in RTT. SRB1 can be modulated by either exogenous or endogenous OS [9] and the presence of chronic OS has been well documented in *CDKL5* with a strong correlation between the levels of OS markers and disease severity [11]. We suggest that the loss of SRB1 is most likely due to the oxidative posttranslational modifications observed as HNE adducts and NT modification of SRB1. The discrepancy between mRNA and protein expression of SRB1 in *CDKL5* fibroblasts leads us to conclude that the loss of protein is not at the transcriptional level, but can be the consequence of posttranscriptional events. Thus, the upregulation of SRB1 mRNA may represent an attempted compensatory mechanism for the increased protein turnover (positive feedback). It should also be mentioned that elevated mRNA levels of proteins that have been damaged by oxidative stress could also depend on an altered translation process by affecting ribosomal proteins and leading to protein misfolding. Indeed, when cells are exposed to OS, several targets can be oxidized and many metabolic pathways, such as translation, can be corrupted [30]. For instance, it has been demonstrated that OS is able to inactivate several enzymes involved in the metabolism of energy and amino acid synthesis [31], which are involved in protein synthesis. Furthermore, several players that participate in translation have been found to be targets of oxidation, including elongation factors, ribosomal proteins, tRNA, and aminoacyl-tRNA synthetases [32]. We do not exclude that some of these pathways also contribute to the detected discrepancy between SRB1 mRNA and protein levels.

In fact, we have previously shown that SRB1 is susceptible to HNE adducts and this leads to its ubiquitination and then to its degradation via the proteasomal machinery [10,33], and this is in line with the data presented in this work. In addition, our results are in line with our previous work showing increased HNE–PA plasma levels in *CDKL5* patients [11].

We should also mention that SRB1 can be regulated at the transcriptional level by several factors (LXRs, SREBP, PPAR, miRNAs, etc.), which could also be involved in our system although there are no data in the literature on the possible SRB1 transcriptional regulation in RTT.

Several defensive pathways can be activated by cells against OS. Among these, there is the activation of the redox-sensitive transcription factor Nrf2, able to regulate the expression of many "antioxidant" genes and other cytoprotective phase II detoxifying enzymes through binding to EpRE's [12–14]. Moreover, recent work has also demonstrated that Nrf2 can be involved in the regulation of proteasome subunits [34]. In addition, it has also been reported that proteasome inhibitors can protect cells and tissues against oxidative damage, because they can activate the Nrf2 pathway [35–37]. In line with the above-mentioned studies, our data showed that Nrf2 translocation in *CDKL5* cells was significantly lower than in the control, once challenged with H_2O_2 or HNE, suggesting the inability of *CDKL5* cells to induce a proper defensive response, as also demonstrated by the *GCLC* data. Moreover, it is likely that *CDKL5* cells exhibit an impaired protein degradation/turnover, resulting in increased accumulation of oxidatively modified proteins.

In addition, Nrf2 is also a regulator of the aldo-keto reductase AKR1C1 [38]. AKR1C1-mediated reduction of HNE has been reported in human hepatoma HepG2 cells and astrocytes [39,40]. Therefore, AKR1C1 is involved in the protection of cells against HNE toxicity and it is logical to suppose that the lower level of Nrf2 in *CDKL5* cells is also responsible for the inability to prevent deleterious effects of HNE. Furthermore, the increased levels of NT can be explained by the induction of iNOS and these results are in line with a recent study that demonstrated the increase in NT levels in Nrf2-knockout mice [41]. HNE, in a dose-dependent manner, is also able to induce NO production, as suggested by Gatbonton-Schwager et al., through cross talk between iNOS and Nrf2 [42]. The lower activation of Nrf2 in *CDKL5* could be a consequence of the high levels of HNE, as demonstrated for another redox-sensitive transcription factor, NF-κB. Studies have shown that low concentrations of HNE (~1 μM) can promote IκB-α phosphorylation, leading to NF-κB activation [43,44]. In contrast, higher concentrations of HNE (5–50 μM) inhibit IκB-α degradation via the proteasome [43,45].

In conclusion, the present work demonstrated a close similarity between typical RTT and *CDKL5* disorder in terms of serum cholesterol levels and SRB1 posttranslational modifications. The loss of SRB1 can be associated with increased lipoproteins found in the serum of *CDKL5* patients and may be the consequence of increased levels of HNE and ubiquitin adducts. This is the first report showing in *CDKL5* patients an increase in both oxidative and nitrosative stress markers and a Nrf2 aberrant activation, all factors that can contribute to cell damage (Scheme 1).

This work demonstrates a novel mechanism in *CDKL5* pathology and a common denominator between two RTT variants, suggesting new insights for possible therapeutic targets that may contribute to improving the quality of life for these patients.

Acknowledgments

Abbreviations

CDKL5	cyclin-dependent kinase-like 5
GCLC	glutamate–cysteine ligase catalytic subunit
HNE	4-hydroxy-2-nonenal
HNE–PA	HNE–protein adduct
iNOS	inducible NO synthase
MECP2	methyl-CpG binding protein 2
Nrf2	nuclear factor erythroid 2-related factor 2
NT	nitrotyrosine
NT–PA	NT–protein adduct
RTT	Rett syndrome
SRB1	scavenger receptor class B, type 1

References

1. Rett A. Uberein eigartiges hirnatrophisches Syndrom bei Hyperammoniamie in Kindesalter. Wien Med Wochenschr. 1966; 116:723–728. [PubMed: 5300597]

2. Hagberg B, Aicardi J, Dias K, Ramos O. A progressive syndrome of autism, dementia, ataxia, and loss of purposeful hand use in girls: Rett's syndrome: report of 35 cases. Ann Neurol. 1983; 14:471–479. [PubMed: 6638958]

3. Amir RE, Van den Veyver IB, Wan M, Tran CQ, Francke U, Zoghbi HY. Rett syndrome is caused by mutation in X–linked MECP2, encoding methyl–CpG–binding protein 2. Nat Genet. 1999; 23:185–188. [PubMed: 10508514]

4. Hagberg B. Clinical delineation of Rett syndrome variants. Neuropediatrics. 1995; 26:62. [PubMed: 7566453]

5. Hanefeld F. The clinical pattern of the Rett syndrome. Brain Dev. 1985; 7:320–325. [PubMed: 4061766]

6. Scala E, Ariani F, Mari F, Caselli R, Pescucci C, Longo I, Meloni I, Giachino D, Bruttini M, Hayek G, Zappella M, Renieri A. CDKL5/STK9 is mutated in Rett syndrome variant with infantile spasms. J Med Genet. 2005; 42:103–107. [PubMed: 15689447]

7. [Accessed 11 July 2014] http://www.cdkl5.com/For-Families/FAQ.aspx

8. Buchovecky CM, Turley SD, Brown HM, Kyle SM, McDonald JG, Liu B, Pieper AA, Huang W, Katz DM, Russell DW, Shendure J, Justice MJ. A suppressor screen in Mecp2 mutant mice implicates cholesterol metabolism in Rett syndrome. Nat Genet. 2013; 45:1013–1020. [PubMed: 23892605]

9. Valacchi G, Sticozzi C, Lim Y, Pecorelli A. Scavenger receptor class B type I: a multifunctional receptor. Ann N Y Acad Sci. 2011; 1229:E1–E7. [PubMed: 22239457]

10. Sticozzi C, Belmonte G, Pecorelli A, Cervellati F, Leoncini S, Signorini C, Ciccoli L, De Felice C, Hayek J, Valacchi G. Scavenger receptor B1 post-translational modifications in Rett syndrome. FEBS Lett. 2013; 587:2199–2204. [PubMed: 23711372]

11. Pecorelli A, Ciccoli L, Signorini C, Leoncini S, Giardini A, D'Esposito M, Filosa S, Hayek J, De Felice C, Valacchi G. Increased levels of 4HNE-protein plasma adducts in Rett syndrome. Clin Biochem. 2011; 44:368–371. [PubMed: 21276437]

12. Motohashi H, Yamamoto M. Nrf2-Keap1 defines a physiologically important stress response mechanism. Trends Mol Med. 2004; 10:549–557. [PubMed: 15519281]

13. Lee JM, Johnson JA. An important role of Nrf2-ARE pathway in the cellular defense mechanism. J Biochem Mol Biol. 2004; 37:139–143. [PubMed: 15469687]

14. Zhang DD. Mechanistic studies of the Nrf2-Keap1 signaling pathway. Drug Metab Rev. 2006; 38:769–789. [PubMed: 17145701]

15. Ma Q. Role of Nrf2 in oxidative stress and toxicity. Annu Rev Pharmacol Toxicol. 2013; 53:401–426. [PubMed: 23294312]

16. Auburger G, Klinkenberg M, Drost J, Marcus K, Morales-Gordo B, Kunz WS, Brandt U, Broccoli V, Reichmann H, Gispert S, Jendrach M. Primary skin fibroblasts as a model of Parkinson's disease. Mol Neurobiol. 2012; 46:20–27. [PubMed: 22350618]

17. Valacchi G, Pecorelli A, Mencarelli M, Carbotti P, Fortino V, Muscettola M, Maioli E. Rottlerin: a multifaced regulator of keratinocyte cell cycle. Exp Dermatol. 2009; 18:516–521. [PubMed: 19492998]

18. Pecorelli A, Bocci V, Acquaviva A, Belmonte G, Gardi C, Virgili F, Ciccoli L, Valacchi G. NRF2 activation is involved in ozonated human serum upregulation of HO-1 in endothelial cells. Toxicol Appl Pharmacol. 2013; 267:30–40. [PubMed: 23253326]

19. Pecorelli A, Leoni G, Cervellati F, Canali R, Signorini C, Leoncini S, Cortelazzo A, De Felice C, Ciccoli L, Hayek J, Valacchi G. Genes related to mitochondrial functions, protein degradation, and chromatin folding are differentially expressed in lymphomonocytes of Rett syndrome patients. Mediators Inflamm. 2013; 2013:137629. [PubMed: 24453408]

20. Höhn A, König J, Grune T. Protein oxidation in aging and the removal of oxidized proteins. J Proteomics. 2013; 92:132–159. [PubMed: 23333925]

21. Pickering AM, Davies KJ. Degradation of damaged proteins: the main function of the 20S proteasome. Prog Mol Biol Transl Sci. 2012; 109:227–248. [PubMed: 22727423]

22. Wild AC, Moinova HR, Mulcahy RT. Regulation of gamma-glutamylcysteine synthetase subunit gene expression by the transcription factor Nrf2. J Biol Chem. 1999; 274:33627–33636. [PubMed: 10559251]

23. Bahi-Buisson N, Nectoux J, Rosas-Vargas H, Milh M, Boddaert N, Girard B, Cances C, Ville D, Afenjar A, Rio M, Héron D, N'guyen Morel MA, Arzimanoglou A, Philippe C, Jonveaux P, Chelly J, Bienvenu T. Key clinical features to identify girls with CDKL5 mutations. Brain. 2008; 131:2647–2661. [PubMed: 18790821]

24. Mari F, Azimonti S, Bertani I, Bolognese F, Colombo E, Caselli R, Scala E, Longo I, Grosso S, Pescucci C, Ariani F, Hayek G, Balestri P, Bergo A, Badaracco G, Zappella M, Broccoli V, Renieri A, Kilstrup-Nielsen C, Landsberger N. CDKL5 belongs to the same molecular pathway of MeCP2 and it is responsible for the early-onset seizure variant of Rett syndrome. Hum Mol Genet. 2005; 14:1935–1946. [PubMed: 15917271]

25. Livide G, Patriarchi T, Amenduni M, Amabile S, Yasui D, Calcagno E, Lo Rizzo C, De Falco G, Ulivieri C, Ariani F, Mari F, Mencarelli MA, Hell JW, Renieri A, Meloni I. GluD1 is a common altered player in neuronal differentiation from both MECP2-mutated and CDKL5-mutated iPS cells. Eur J Hum Genet. 2015; 23:195–201. [PubMed: 24916645]

26. Orth M, Bellosta S. Cholesterol: its regulation and role in central nervous system disorders. Cholesterol. 2012; 2012:292598. [PubMed: 23119149]

27. Brown WE, Rodwell VW. Hydroxymethylglutaryl-CoA reductase. Experientia Suppl. 1980; 36:232–272. [PubMed: 6987078]

28. Pallottini V, Martini C, Bassi AM, Romano P, Nanni G, Trentalance A. Rat HMGCoA reductase activation in thioacetamide-induced liver injury is related to an increased reactive oxygen species content. J Hepatol. 2006; 44:368–374. [PubMed: 16140414]

29. Segatto M, Trapani L, Di Tunno I, Sticozzi C, Valacchi G, Hayek J, Pallottini V. Cholesterol metabolism is altered in rett syndrome: a study on plasma and primary cultured fibroblasts derived from patients. PLoS One. 2014; 9:e104834. [PubMed: 25118178]

30. Grant CM. Regulation of translation by hydrogen peroxide. Antioxid Redox Signal. 2011; 15:191–203. [PubMed: 21126188]

31. Bulteau AL, Szweda LI, Friguet B. Mitochondrial protein oxidation and degradation in response to oxidative stress and aging. Exp Gerontol. 2006; 41:653–657. [PubMed: 16677792]

32. Katz, A., Orellana, O. Protein synthesis and the stress response. In: Biyani, M., editor. Cell-free protein synthesis. InTech; Rijeka: 2012. p. 111-134.

33. Sticozzi C, Belmonte G, Pecorelli A, Arezzini B, Gardi C, Maioli E, Miracco C, Toscano M, Forman HJ, Valacchi G. Cigarette smoke affects keratinocytes SRB1 expression and localization via H2O2 production and HNE protein adducts formation. PLoS One. 2012; 7:e33592. [PubMed: 22442701]

34. Pickering AM, Linder RA, Zhang H, Forman HJ, Davies KJ. Nrf2-dependent induction of proteasome and Pa28αβ regulator are required for adaptation to oxidative stress. J Biol Chem. 2012; 287:10021–10031. [PubMed: 22308036]

35. Dreger H, Westphal K, Weller A, Baumann G, Stangl V, Meiners S, Stangl K. Nrf2-dependent upregulation of antioxidative enzymes: a novel pathway for proteasome inhibitor-mediated cardioprotection. Cardiovasc Res. 2009; 83:354–361. [PubMed: 19351736]

36. Duan W, Guo Y, Jiang H, Yu X, Li C. MG132 enhances neurite outgrowth in neurons overexpressing mutant TAR DNA-binding protein-43 via increase of HO-1. Brain Res. 2011; 1397:1–9. [PubMed: 21620381]

37. Luo ZF, Qi W, Feng B, Mu J, Zeng W, Guo YH, Pang Q, Ye ZL, Liu L, Yuan FH. Prevention of diabetic nephropathy in rats through enhanced renal antioxidative capacity by inhibition of the proteasome. Life Sci. 2011; 88:512–520. [PubMed: 21241714]

38. Jung KA, Choi BH, Nam CW, Song M, Kim ST, Lee JY, Kwak MK. Identification of aldo-keto reductases as NRF2-target marker genes in human cells. Toxicol Lett. 2013; 218:39–49. [PubMed: 23305850]

39. Burczynski ME, Sridhar GR, Palackal NT, Penning TM. The reactive oxygen species–and Michael acceptor-inducible human aldo-keto reductase AKR1C1 reduces the alpha,beta-unsaturated aldehyde 4-hydroxy-2-nonenal to 1,4-di-hydroxy-2-nonene. J Biol Chem. 2001; 276:2890–2897. [PubMed: 11060293]

40. Malone PE, Hernandez MR. 4-Hydroxynonenal, a product of oxidative stress, leads to an antioxidant response in optic nerve head astrocytes. Exp Eye Res. 2007; 84:444–454. [PubMed: 17173895]

41. McGrath-Morrow S, Lauer T, Yee M, Neptune E, Podowski M, Thimmulappa RK, O'Reilly M, Biswal S. Nrf2 increases survival and attenuates alveolar growth inhibition in neonatal mice exposed to hyperoxia. Am J Physiol Lung Cell Mol Physiol. 2009; 296:L565–L573. [PubMed: 19151108]

42. Gatbonton-Schwager TN, Sadhukhan S, Zhang GF, Letterio JJ, Tochtrop GP. Identification of a negative feedback loop in biological oxidant formation fegulated by 4-hydroxy-2-(E)-nonenal. Redox Biol. 2014; 2:755–763. [PubMed: 25009777]

43. Poli G, Schaur RJ, Siems WG, Leonarduzzi G. 4-hydroxynonenal: a membrane lipid oxidation product of medicinal interest. Med Res Rev. 2008; 28:569–631. [PubMed: 18058921]

44. Ruef J, Moser M, Bode C, Kübler W, Runge MS. 4-hydroxynonenal induces apoptosis, NF-kappaB-activation and formation of 8-isoprostane in vascular smooth muscle cells. Basic Res Cardiol. 2001; 96:143–150. [PubMed: 11327332]

45. Ji C, Kozak KR, Marnett LJ. IkappaB kinase, a molecular target for inhibition by 4-hydroxy-2-nonenal. J Biol Chem. 2001; 276:18223–18228. [PubMed: 11359792]
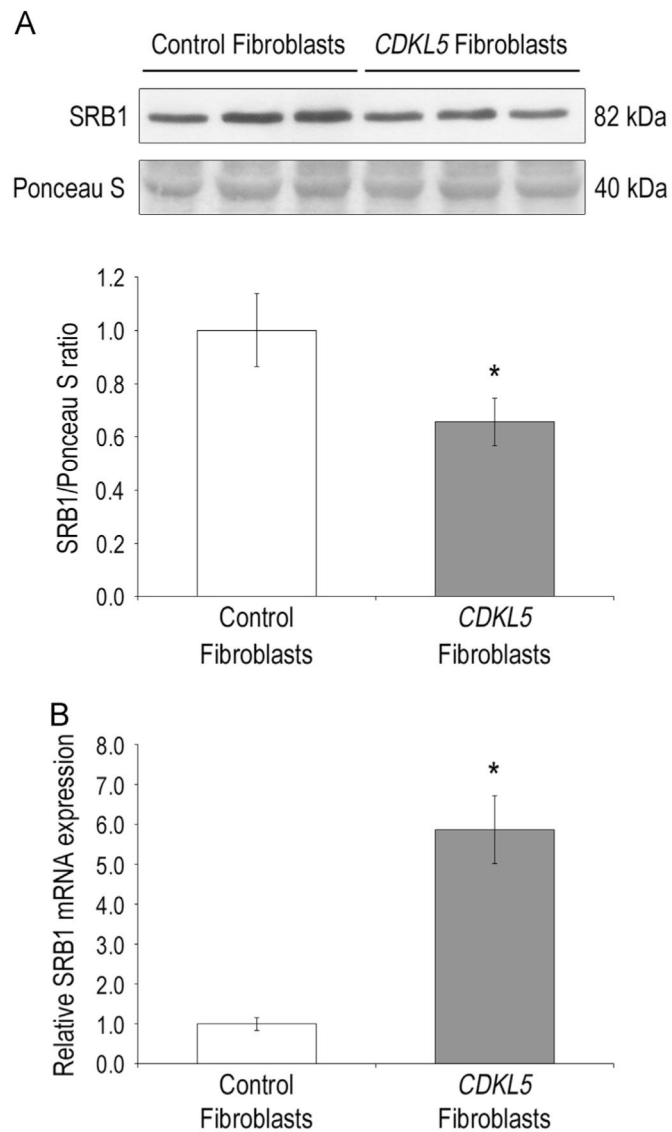
Fig. 1.
SRB1 protein and mRNA expression in *CDKL5* fibroblasts. (A) Top, a representative Western blot of SRB1 in healthy control (*n*=4) and *CDKL5* (*n*=4) fibroblasts is shown. Bottom, the relative SRB1 levels normalized to a Ponceau-stained band around 40 kDa. Values are reported as arbitrary units. Data are means±SD of three separate experiments. *P<0.05. (B) The relative levels of SRB1 mRNA expression in healthy control (*n*=4) and *CDKL5* (*n*=4) fibroblasts, as quantified by RT-qPCR. Data are the means±SEM of three independent experiments, each analyzed in triplicate. The SRB1 mRNA is normalized to GAPDH and expressed as a fold change. *P<0.05.

Fig. 2.
CDKL5 fibroblasts show increased oxidative stress markers, i.e., 4-hydroxy-2-nonenal–
protein adducts, nitrotyrosine–protein adducts, and overexpression of iNOS. (A)
Representative Western blots for HNE–PA (left) and NT–PA (right) in healthy control (*n*=4)
and *CDKL5* (*n*=4) fibroblasts are shown. HNE–PA were present between 50 and 250 kDa,
and bands reactive for NT–PA were observed in the range of 50 to 100 kDa. At the bottom is
presented the Western blot quantification. (B) Immunofluorescence for HNE–PA (red) and
NT–PA (green) in control and *CDKL5* fibroblasts. Original magnification, ×630. Scale bar,
50 μm, valid for all images. (C) Left, a representative Western blot of iNOS protein levels in
healthy control (*n*=4) and *CDKL5* (*n*=4) fibroblasts. Right, quantification of the iNOS

Western blot. Values are reported as arbitrary units. Data are means±SD of at least three independent experiments. *$P<0.05$.
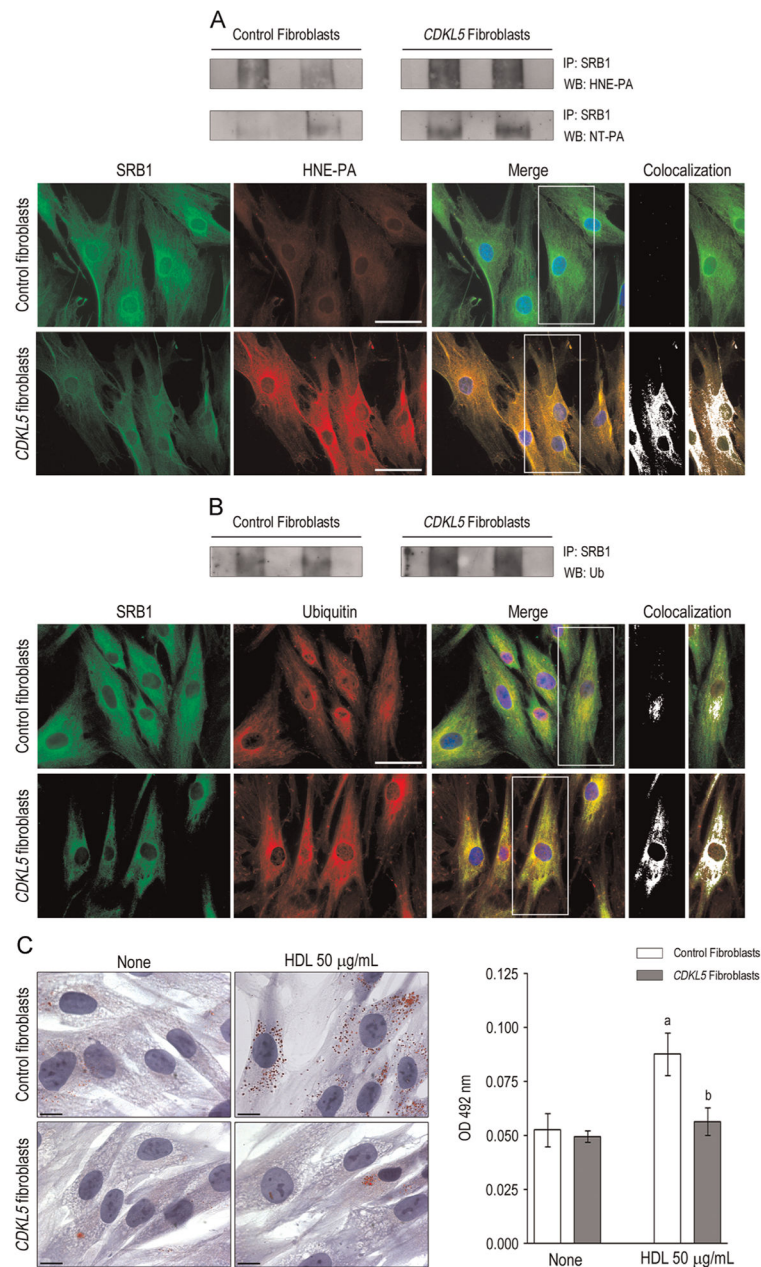
Fig. 3.

SRB1 posttranslational modifications and cholesterol uptake in *CDKL5* fibroblasts. (A) Representative immunoblotting of HNE and NT for immunoprecipitated SRB1 in control (*n*=4) and *CDKL5* (*n*=4) fibroblasts (top). Bottom, double immunofluorescence shows the presence of SRB1 (green fluorescence), HNE–PA (red fluorescence), and HNE–SRB1 adducts (yellow) in healthy control and *CDKL5* fibroblasts. In the merged images, white spots indicate the clear colocalization of SRB1 with HNE in *CDKL5* fibroblasts. Original magnification, ×630. Scale bar, 50 μm. (B) Representative immunoblotting of ubiquitin after SRB1 immunoprecipitation. Control (*n*=4) and *CDKL5* (*n*=4) fibroblasts (top). Bottom, double immunofluorescence shows the presence of SRB1 (green fluorescence), ubiquitin

(red fluorescence), and ubiquitin–SRB1 adducts (yellow) in healthy control and *CDKL5* fibroblasts. In the merged images, white spots indicate the clear colocalization of SRB1 with ubiquitin in *CDKL5* fibroblasts. Original magnification, ×630. Scale bar, 50 μm. (C) Representative images of oil red O staining show a reduced number of cellular lipid droplets in *CDKL5* fibroblasts exposed to HDL (50 μM) for 24 h (left). Original magnification, ×1000. Scale bars, 10 μm. Right, histogram shows quantification of HDL-cholesterol uptake. Values are reported as optical density at 492 nm, normalized to protein concentration. Data are means±SD of three separate experiments. [a]P<0.05 between treated and not treated samples; [b]P<0.05 between control and *CDKL5 treated samples.*
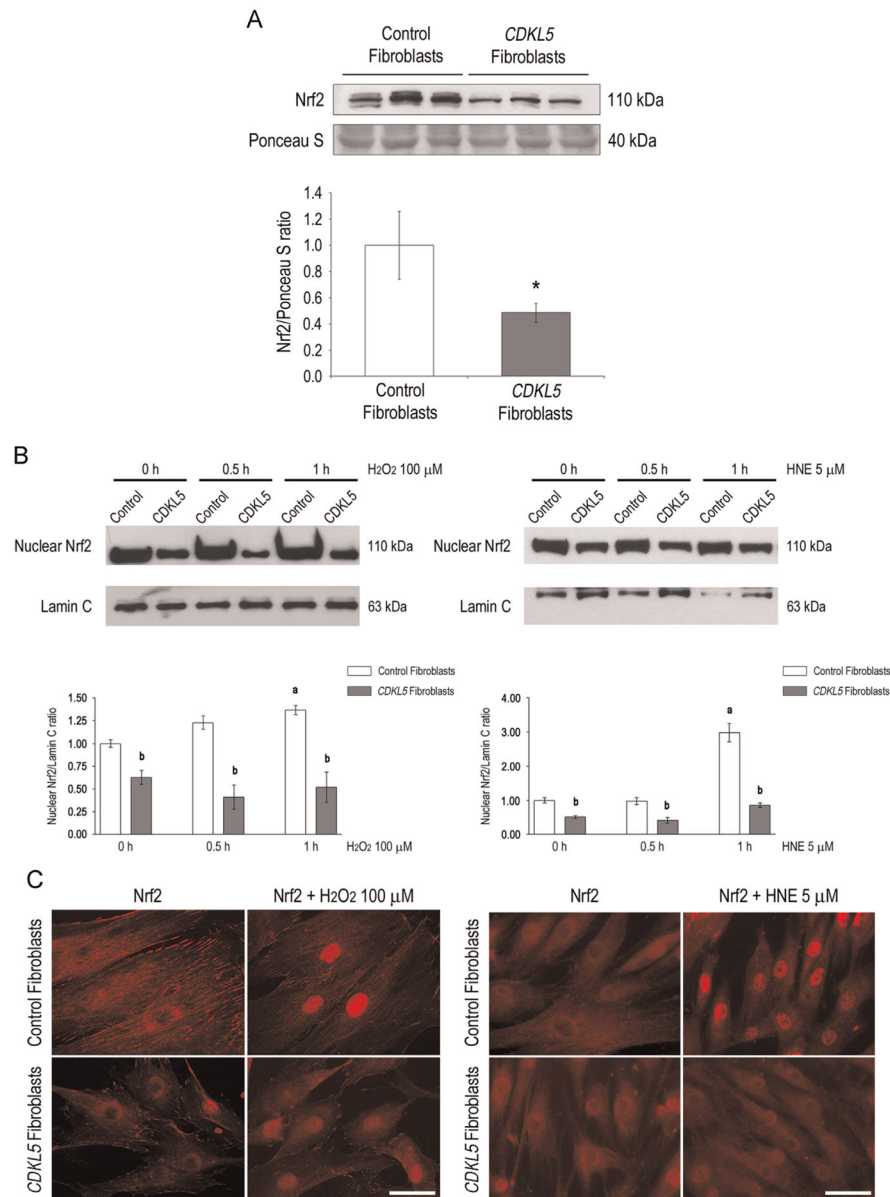
Fig. 4.
Levels and nuclear translocation of Nrf2. (A) Top, representative Western blot for Nrf2 in healthy control (n=4) and *CDKL5* (n=4) fibroblasts. Bottom, the Western blot quantification. Values are reported as arbitrary units. Data are means±SD of at least three separate experiments. *P<0.05. (B) Representative Western blot for Nrf2 nuclear translocation in healthy control (n=4) and *CDKL5* (n=4) fibroblasts challenged with H_2O_2 (left) or HNE (right) at various time points. Bottom, quantification of Nrf2 nuclear levels relative to lamin C. Values are reported as arbitrary units. Data are means±SD from three separate experiments. [a]P<0.05 in the same group; [b]P<0.05 between control and *CDKL5*. (C) Representative images of immunofluorescence for Nrf2 nuclear translocation in healthy control and *CDKL5* fibroblasts treated with H_2O_2 (left) or HNE (right) for 1 h. Original magnification, ×630. Scale bar, 50 μm, valid for all images.
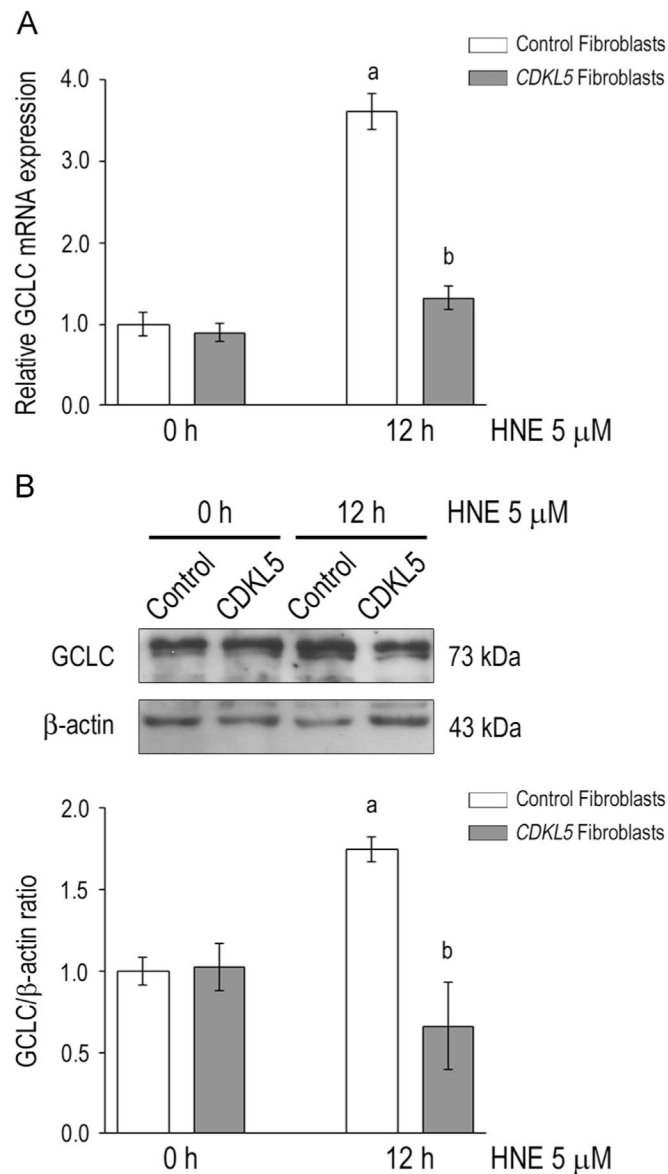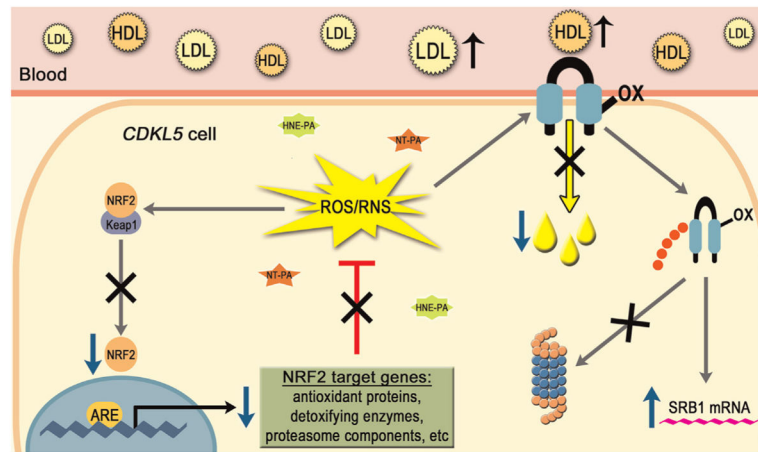
Fig. 5.
GCLC mRNA and protein levels in *CDKL5* and healthy fibroblasts. (A) Basal and HNE-stimulated levels of GCLC mRNA expression in healthy control (n=4) and *CDKL5* (n=4) fibroblasts. Data are the means±SEM of three independent experiments, each analyzed in triplicate. The GCLC mRNA is normalized to GAPDH and expressed as a fold change. [a]P<0.05 in the same group; [b]P<0.05 between control and *CDKL5 treated samples.* (B) Representative Western blot for GCLC protein levels in healthy control (n=4) and *CDKL5* (n=4) fibroblasts challenged with HNE for 12 h. Bottom, the Western blot quantification. The values are reported as arbitrary units. Data are means±SD of three separate experiments. [a]P<0.05 in the same group; [b]P<0.05 between control and *CDKL5 treated samples.*

Scheme 1.

Several mechanisms can play a role in *CDKL5* disorder, such as redox imbalance and altered cholesterol pathway, two possible common denominators between typical RTT and *CDKL5* patients. Owing to a possible Nrf2 aberrant activation with a defective expression of Nrf2 target genes (detoxifying enzymes, etc.), in *CDKL5* cells the redox imbalance can contribute to the loss of SRB1 as a consequence of increased oxidative modifications and ubiquitin adduct formation in SRB1 protein. In addition, the decrease in SRB1 levels is associated with the reduction in intracellular lipid uptake and the increase in serum lipoproteins found in *CDKL5* patients. Finally, a possible positive feedback loop can be the cause of the SRB1 mRNA overexpression. ARE, antioxidant-response element.

Table 1

Comparison of serum lipid profiles between healthy normal controls and *CDKL5* patients.

	Healthy controls	***CDKL5* patients**	**Student's *t* test *P* value**
TC (mg/dl)	162.3±14.6	194.6±24.7	0.00001
TG (mg/dl)	80.2±20.2	88.9±33.8	0.32674
LDL-C (mg/dl)	87.6±11.3	103.5±16.4	0.04037
HDL-C (mg/dl)	49.8±6.3	67.9±17.9	0.00303
Total number	30	16	—

The values are expressed as means±SD. Abbreviations: TC, total cholesterol; TG, triglycerides; LDL-C, low-density lipoprotein cholesterol; HDL-C, high-density lipoprotein cholesterol.